Section A-Research paper

Recent advances in metal complexes of new multifunctional ether ligand as potential anti-breast cancer agents

Abdou S. El-Tabl*[a], Moshira M. Abd-El Wahed[b], Ahmed M.Ashour[a] , Abdelhaleam Abdelbaky Aly[a] ,Mohammed H. H. Abu-Setta [*a]

[a]Department of Chemistry, Faculty of Science, El-Menoufia University, Shebin El -Kom, Egypt.
[b]Department of Pathology, Faculty of Medicine, El-Menoufia University, Shebin El-Kom, Egypt.

ABSTRACT

There has been much interesting in the development a new ether Schiff-base ligand and its Co(II), Ni(II), Cu(II), Zn(II), Mn(II) and Ag(I), complexes as antitumor agents . Ligand and its complexes have been characterized by elemental analysis, IR, UV-Vis spectra , ^{1}H-NMR spectra, Mass spectra, Magnetic moments, Conductances, Thermal analyses (DTA and TGA) and ESR measurements The spectral data showed that, the ligand behaved a neutral hexadentate type. Molar conductance's in DMF solution indicated non-electrolytic nature of the prepared complexes. The ESR spectra of the solid complexes indicated anisotropic or isotropic type (dx^2-y^2) ground state with considerable covalent bond character. Electron microscopic data [TEM] indicated that, the complexes under study were in nanoparticles (NP_s) from (7.18-82.4 nm). The cytotoxicity of the ligand and some of its metal complexes against human breast cancer cell (MCF-7 cell line) have been carried out. Complex (8) showed high toxicity, the order of cytotoxic effect against MCF-7 cell line were Cu(II)/Zn(II) complex (8)>Cisplatin>Cu(II) complex (2)>Ligand (1) at all concentrations were used. The cells were dosed with the complexes at varying concentrations and cell viability was measured by sulfo-rhodamine-B stain (SRB) method. These compounds which were mentioned above showed marked antiproliferative effect compared with standard drug (Cisplatin) used.

Keywords: Schiff base ligand, cytotoxicity complexes, spectra, magnetism, breast cancer.

INTRODUCTION

Recently considerable attention have been given to Schiff bases complexes due to not only for coordination chemistry but for pharmacological applications, were, due to their good complexes properties and significant biological activity [1,2]. Chemistry of transition metal complexes of Schiff bases became largely appealing because of their broad profile of pharmacological activity that provides a diverse variety of compounds with different activities [3]. Some of the detected biological activities of the Schiff bases and their complexes with transition metal ions are antibacterial, antifungal, antiarthritic, antimalarial, antitumor, antiviral and anti-HIV activities [4-6]. Schiff bases derivatives containing a 4-acyl-2-pyrazolin-5- one moiety form an important class of organic compounds were due to their structural chemistry and biological activities [7,8]. In the field of anticancer research, the pyrazolones exhibited promising antiproliferative activity against human myelogenous leukaemia HL-606. The coordinating property of the 4-amino-2,3-dimethyl-1-phenyl-3-pyrazolin-5-one ligand had been modified to give a flexible ligand system, formed by condensation with a variety of reagents such as aldehydes, ketones [9-

[11], and carbazides [12-14]. The biological properties of Schiff bases are often related and modulated by metal ion coordination [15-18]. Cu(II), Ni(II) and Co(II) complexes of Schiff base derived from 4,6-diacetyl resorcinol had been prepared and spectroscopically characterized [19]. New multifunctional ether ligand and its metal complexes, also antibreast activity of some compounds have been studied. This article involved preparation and spectroscopically characterization.

MATERIALS AND METHODS

All the reagents employed for the preparation of the ligand and its complexes were synthetic grade and used without further purification. TLC is used to confirm the purity of the prepared complexes. C, H, N and Cl analyses were determined at the Analytical Unit of Cairo University, Egypt. Standard gravimetric methods were used to determine metal ions [20-22]. All metal complexes were dried under vacuum over P_4O_{10}. The IR spectra were measured as KBr pellets using a Perkin-Elmer 683 spectrophotometer (4000-400 cm^{-1}). Electronic spectra (qualitative) DMF were recorded on a Perkin-Elmer 550 spectrophotometer. The conductances(10^{-3}M) of the complexes in DMF were measured at 25 °C with a Bibby conduct meter type MCl. ^{1}H-NMR spectra of the ligand and its Ag(I),and Zn(II)/Cu(II) complex were obtained with Perkin-Elmer R32-90-MHz spectrophotometer using TMS as internal standard. Mass spectra were recorded using JEULJMS-AX-500 mass spectrometer provided with data sys-tem. The thermal analyses (DTA and TGA) were carried out in air on a Shimadzu DT-30 thermal analyzer from 27 to 700 °C at a heating rate of 10 °C per minute. Magnetic susceptibilities were measured at 25 °C by the Gouy method using mercuric tetrathiocyanatocobalt (II) as the magnetic susceptibility standard.

Diamagnetic corrections were estimated from Pascal's constant. The magnetic moments were calculated from the equation:

$$\mu_{eff.} = 2.84\sqrt{\chi_M^{corr}.T}\ .$$

The ESR spectra of solid complexes at room temperature were recorded using a varian E-109 spectrophotometer; DPPH was used as a standard material. Transmission electron microscopic samples were prepared by dropping the colloids onto carbon-coated TEM grids and allowed the liquid carrier to evaporate in air then assayed by a JEOL1230transimishion electron microscope (120KV).

Preparation of compound (I) and compound (II):

Dimethyl 4,4'-(butane-1,4-diylbis(oxy))dibenzoate and 4,4'-(butane-1,4-diylbis(oxy))di(benzohydrazide)

Compound I (Scheme 1) was prepared by adding of dibromoethane (1.87 ml, 0.01 mol), to methyl-p-hydroxybenzoate sodium salt (2.49 g, 0.02 mol) dissolved in 50 cm^3 of absolute ethanol. Warming with stirring for one hour to give the product. Compound (II) was prepared by dissolving two moles of hydrazine hydrate (1.0012 g) dissolved in 50 cm^3 of absolute ethanol and added it to compound (I). The mixture was refluxed on water bath for one hour and then left to cool at room temperature, filtered off, the formed precipitate was washed with distilled water, dried and recrystallized from ethanol to afford dimethyl 4,4'-(butane-1,4-diylbis(oxy))dibenzoate and 4,4'-(butane-1,4-diylbis(oxy))di(benzohydrazide); compound (II).

Preparation of the Schiff-base ligand (1)[H_4L] (Z)-N'-(2-hydroxybenzylidene)-4-(2-(4-((E)-2-(2hydroxybenzylidene)hydrazinecarbonyl)phenoxy)ethoxy benzohydrazide

H_4L (Scheme 1) was prepared by adding two moles of salysaldehyde (1.22 g, 0.01 mol) to one mole of compound (II), (4,4'-(butane-1,4-diylbis(oxy))di(benzohydrazide) (3.30 g, 0.01 mol) dissolved in 50 cm3 of absolute ethanol The mixture was refluxed with stirring for 3 hours. The dark product which formed was filtrated off and washed with distilled water and dried in air to give brown product. Then it was recrystallized from ethanol to give a pure needle shaped crystals of (H_4L),(1).

Synthesis of metal complexes (2)-(11):

A filtered ethanoic (50 cm^3) of $Cu(OAc)_2$. H_2O (0.6 g, 0.003 mol) was added to an ethanolic (50 cm^3) of the ligand, **(1)** (1.8 g, 0.003 mol) [1L:2M], complex **(2), (**1.28 g, 0.005 mol) $Ni(OAc)_2.4H_2O$, [1L:2M], complex **(3),** (3.41 g, 0.014 mol) of $Co(OAc)_2.4H_2O$ [1L:2M], complex **(4),** (6.15 g, 0.028 mol) of $Zn(OAc)_2.2H_2O$ [1L:2M] complex **(5),** (6.84 g, 0.028 mol) of $Mn(OAc)_2.2H_2O$, [1L:2M], complex **(6),** (2.70 g, 0.016 mol) $Ag(OAc)_2$. H_2O, [1L:2M], complex **(7)**, (3 g, 0.014 mol) of $Zn(OAc)_2.2H_2O$ and (2.4 g, 0.013 mol) of $Cu(OAc)_2$. H_2O , [1L:2M], complex **(8),** (3.0 g, 0.014 mol) of $Zn(OAc)_2.2H_2O$ and (3.45 g, 0.014 mol) of $Co(OAc)_2.4H_2O$, [1L:2M], complex **(9) ,** (5.60 g, 0.024 mol) of $CuSO_4.5H_2O$, [1L:2M], complex **(10**), (5.75 g, 0.027 mol) of $CuCl_2.2H_2O$, [1L:2M], complex **(11**),. The mixture was refluxed with stirring for 1-3 hrs range, depending on the nature of metal salts, the coloured complex which formed was filtered off, washed with ethanol and dried under vacuum over P_4O_{10}.

Scheme1: preparation of [H_4L] (1)

Table 1. Analytical and physical data of $[H_4L]$,**(1)** and it's metal complexes:

$^{*}Ohm^{-1}\ cm^{2}\ mol^{-1}$

No.	Ligand 1 and Complexes	Color	FW	M.P (^{o}C)	Yield (%)	Anal. /Found (Calc.) (%)					Molar conductance (Λ_m)*
						C	H	N	M	Cl	
(1)	$[(H_4L)$ $C_{29}H_{24}N_4O_6$	brown	524.52	>300	88	66.11(66.41)	4.15(4.61)	10.04(10.68)	-	-	0.2
(2)	$[(H_4L)(Cu)_2(OAc)_4(H_2O)_2].H_2O$ $C_{37}H_{42}Cu_2N_4O_{17}$	faint oily	941.84	>300	78	46.82 (47.18)	4.72 (4.49)	5.78 (5.95)	13.28 (13.49)	-	7.56
(3)	$[(H_4L)$ $(Ni)_2(OAc)_4(H_2O)_2].2H_2O$ $C_{37}H_{44}N_4Ni_2O_{18}$	Dark gray	950.15	>300	75	45.99 (46.77)	4.59 (4.67)	5.77 (5.90)	12.25 (12.35)	-	6.38
(4)	$[(H_4L)(Co)_2(OAc)_4(H_2O)_2].2H_2O$ $C_{37}H_{40}Co_2N_4O_{16}$	gray	914.60	>300	77	48.21 (48.59)	4.32 (4.41)	5.98 (6.13)	12.74 (12.89)	-	8.2
(5)	$[(H_4L)$ $(Zn)_2(OAc)_4(H_2O)_2].2H_2O$ $C_{37}H_{44}N_4O_{18}Zn_2$	Dark gray	963.52	>300	75	45.66 (46.12)	4.58 (4.60)	5.62 (5.81)	13.40 (13.57)	-	9.0
(6)	$[(H_4L)$ $(Mn)_2(OAc)_4(H_2O)_2].3H_2O$ $C_{37}H_{46}Mn_2N_4O_{19}$	faint oily	960.56	>300	77	46.12(46.26)	3.94(4.83)	(5.83) 5.79	11.12 (11.44)	-	8.7
(7)	$[(H_4L)$ $(Ag)_2(OAc)_2(H_2O)_2].H_2O$ $C_{37}H_{40}Ag_2N_4O_{16}$	gray	1012.5	>300	82	41.79 (41.53)	4.25 (4.17)	5.91 (5.73)	22.75 (22.31)	-	7.63
(8)	$[(H_4L)(Cu)(Zn)(OAc)_4(H_2O)_2].2H_2O$ $C_{37}H_{44}N_4O_{18}CuZn$	Faint green	961.69	>300	80	45.28 (46.21)	3.96 (4.61)	5.82 (5.83)	13.53 (13.41)	-	7.8
(9)	$[(H_4L)(Co)(Zn)(OAc)_4(H_2O)_2].2H_2O$ $C_{37}H_{44}N_4O_{18}CoZn$	Dark oily	957.07	>300	70	45.47 (46.43)	4.56 (4.63)	5.25 (5.85)	12.25 (12.99)	-	8.2
(10)	$[(H_4L)(Cu)_2(SO_4)_2(H_2O)_4].2H_2O$ $C_{29}H_{36}Cu_2N_4O_{20}S_2$	faint oily	951.83	>300	78	(36.59) 36.30	3.64 (3.81)	5.66 (5.89)	12.41 (13.35)	-	8.0
(11)	$[(H_4L)(Cu)_2(Cl)_4(H_2O)_2].2H_2O$ $C_{29}H_{32}Cl_4Cu_2N_4O_{10}$	brown	865.49	>300	75	(40.24) 40.11	3.31 (3.37)	6.44 (6.47)	(14.68) 14.62	16.32 (16.39)	8.6

BIOLOGICAL ACTIVITY

Cytotoxic activity:

Evaluation of the cytotoxic activity of the ligand and some of its metal complexes was carried out in the Pathology Laboratory, Pathology Department, Faculty of Medicine, El-Menoufia University, Egypt. The evaluation process was carried out invitro using the Sulfo-Rhodamine-B-stain (SRB) assay published method [23]. Cells were plated in 96-multiwell plate (10^4cells/well) for 24 hrs. Before treatment with the complexes to allow attachment of cell to the wall of the plate. Different concentrations of the compounds under test in DMSO (0, 5, 12.5, 25 and 50 µg/ml) were added to the cell monolayer, triplicate wells being prepared for each individual dose. Monolayer cells were incubated with the complexes for 48 hrs.at 37°C using 5% CO_2. After 48 hrs. Cells were fixed, washed and stained with Sulfo-Rhodamine-B-stain. Excess stain was wash with acetic acid and attached stain was recovered with Tri EDTA buffer. Color intensity was measured in an ELISA reader [23]. The relation between surviving fraction and drug concentration is plotted to get the survival curve for each tumor cell line after addition the specified compound**.**

RESULTS AND DISCUSSION

All the complexes are nanoparticles, stable at room temperature, non-hygroscopic, insoluble in water and partially soluble in common organic solvents such as $CHCl_3$, but soluble in DMF and DMSO. The analytical and physical data of the ligand and its complexes were given in Table (1), spectral data (Tables 2-6) were compatible with the proposed structures, Figures (1and 2). The molar conductances in DMF solution were in the 6.3-16.4 $ohm^{-1}cm^2mol^{-1}$ range, Table (1), indicating a non-electrolytic nature [24, 25]. The high value for some complexes suggested partial dissociation in DMF. Reaction of **(1)** with metal salts using (1L: 2M) molar ratios in ethanol gave complexes **(2)-(11)**. The composition of the complexes formed depends on nature of metal salts.

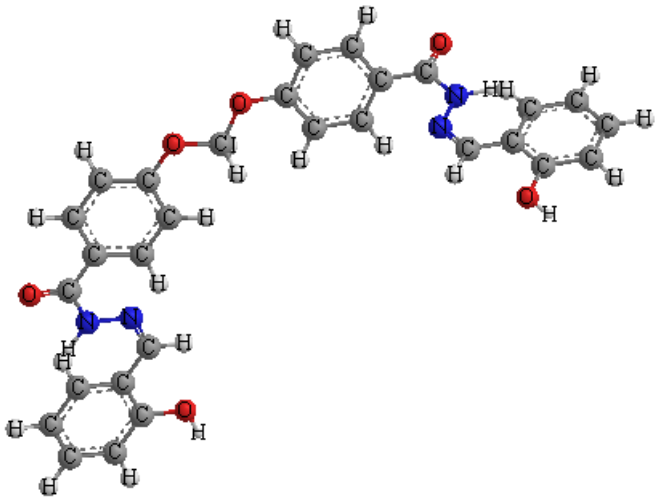

Fig (1): Chemical and 3D structure of Ligand (**1**)

Fig (2): Structure representation of Cu(II), Co(II), Zn(II), Mn(II), and Ag(I) complexes **(2)-(11)**

IR spectra:

The mode of bonding between the ligand and the metal ion explored by comparing the IR spectra of the ligand (**1**) and its metal complexes (**2**)-(**11**). The ligand showed bands in the 3560-3350 and 3340-2980 cm^{-1} ranges, commensurate the presence of two types of intra- and intermolecular hydrogen bonds [26]. Thus, the higher frequency band was associated with a weaker hydrogen bond and the lower frequency corresponded to stronger hydrogen bond. The medium band appeared at 3140 cm^{-1} was assigned to v(NH) group [26,27]. The v(NH) group in the complexes appeared nearly at the same region of the free ligand indicating that, the NH group is not involved in the coordination to the metal ion[28]. The band (NH) appeared at 3125-3160 cm^{-1} range. Strong band observed at 3360 cm^{-1} was attributed to the v(OH) group, it observed in complexes at the region 3480-3420 cm^{-1}.Strong band appeared at 1690 cm^{-1} was due to (C=O) group, it appeared in complexes at the region 1685-1644 cm^{-1},In complexes the bands observed at 3560-3210,and 3370-3820cm^{-1}range,were due to hydrated, coordinated water molecules and hydrogen bondings. Strong band appeared at1625 cm^{-1} was due to v(C=N) band, it observed in all complex at 1601-1620 cm^{-1} range. Acetate ion band v(Ac) appeared at 1449-1320 cm^{-1} range but for complex **(10)** sulphate ion appeared at 1160,1164,1040, and 690 cm^{-1}respectivly , Aromatic bands appeared at two regions, the first observed at 1570-1460 cm^{-1} range and the other band appeared at 815-574 cm^{-1} range for ligand , and appeared in complexes at two regions, the first at 1519-1402 cm^{-1} range, and 771-617cm^{-1} range . Complex (**11**) showed bands in the 420-405 cm^{-1} region was assigned to v(M-Cl). However complexes showed bands in the region 698-521 cm^{-1} range was corresponded to v(M-O), bands observed in the544-422 cm^{-1} range was assigned to v(M-N) [28].

^{1}H-NMR spectra of the ligand (1) and its Ag(I)complex (7)) , and (Zn(II)/Cu(II)) complex (8)

The ^{1}H-NMR spectrum of the ligand showed peak at 7.8 ppm, was due to proton of NH group, and the peaks observed in the 3.5-4.36 ppm range corresponded to protons of methylene groups. The protons of OH aromatic group observed as abroad peak at 10.6 ppm, was due to presence of strong hydrogen bondings, however, the protons of aromatic rings observed at 6.8- 7.5 ppm range and the protons methine group appeared. at 8.8 ppm [29]. The ^{1}H -NMR spectra of the complexes **(7)** and **(8)** showed peaks of NH protons at 7.8 and 7.9 ppm respectively and methylene protons appeared at 3.45-4.47 ppm range. The peaks observed at 10.1 and 10.5 ppm were due to aromatic OH proton, however, the aromatic ring protons appeared at 6.5-7.72 ppm range, finally, The peaks observed at 8.9 and 9.0 ppm were due to protons of methine group respectively [29]. By comparison the ^{1}H- NMR of the ligand and the spectra of complexes, there is a significant downfield shift of the proton signal relative to the free ligand clarified that, the metal ions were coordinated to the ligand.[30, 32]

Mass spectra:

The mass spectra of the ligand **(I)** and its Cu(II) complex **(2)**, and Mn(II) complex **(6)** confirmed their proposed formulations. The spectrum of the ligand revealed the molecular ion peaks (m/z) at 524 amu consistent with the molecular weight of the ligand (524). Furthermore, the fragments observed at (m/z) = 50,65,77,121,223,240,314,390,465, and 524 amu corresponded NH_4O_2,C_4H_3N, C_5H_3N, C_7H_7NO, $C_{12}H_{19}N_2O_2$, $C_{12}H_{20}N_2O_3$, $C_{17}H_{20}N_3O_3$, $C_{22}H_{20}N_3O_4$, $C_{27}H_{20}N_4O_4$, $C_{29}H_{24}N_4O_6$ moieties, respectively. However, the Cu(II) complex **(2)** showed peak (m/z) at 959 amu. Additionally, the peaks observed at (m/z) 60, 93, 121, 185, 371, 562, 599, 661, 740, and 793 amu were due to C_3H_8O, $C_3H_{11}NO_2$,$C_5H_{15}NO_2$, $C_7H_{23}NO_4$, $C_{15}H_{33}NO_9$, $C_{26}H_{33}N_3O_{11}$, $C_{29}H_{34}N_3O_{11}$, $C_{30}H_{36}N_3O_{14}$, $C_{31}H_{40}N_3O_{14}Cu$, $C_{34}H_{41}N_3O_{15}Cu$, and $C_{37}H_{44}N_4O_{18}Cu_2$ moieties, respectively. Finally, the Mn(II) complex **(7)** showed peak (m/z) at 960 amu. The fragments (m/z) observed at 65, 121, 179, 330, 445, 583, 649, 795, and 960 amu were due to Assignments C_3HN_2, $C_5H_3N_2O_2$, $C_7HN_2O_4$, $C_{14}H_4NO_8$, $C_{20}H_{15}NO_{10}$, $C_{24}H_{18}NO_{12}Mn$, $C_{27}H_{20}N_3O_{14}Mn$, $C_{33}H_{30}N_3O_{18}Mn$, and $C_{37}H_{44}N_4O_{18}Mn_2$, moieties, the data are showed in Table (3,i,ii,and iii).

Table 2. IR frequencies of the bands (cm^{-1}) of ligand [H_4L] and its Metal Complexes and their assignments.

	υ(H_2O)	**υ(H-bond.)**	**υ(NH)**	**υ(OH)**	**υ(C=O)**	**υ(C=N)**	**υ(Ar)**	**υ(Oac)/SO4**	**υ(M-O)**	**υ(M-N)**	**υ(M-X)**
(1)	-	3560-3350 3340-2980	3140	3360,1350 1320,422	1690, 1660	1625,612	1570-1460 815-574	-	-	-	-
(2)	3510-3370 3360-3100	3540-2250 3240-2820	3125	3355-3415 1284,1320	1685 1668	1611,1605	1519,1429 676-617	1430,1320	676	544	-
(3)	3500-3360 3350-3060	3540-3260 3250-2750	3130	3355-3470 1281,1316	1680 1644	1605,1600	1530,1513 771,752	1432,1553	667	533	-
(4)	3490-3370 3360-3050	3540-3270 3260-2790	2125	3450,348 3356-1285	1692,1641	1611 1601	1585,1516 768,740	1449,1350	673	519	-
(5)	34703380 3370-3080	3520-3240 3230-2870	3132	3435,1339 3365,1278	1717 1650	1615,1603	1516,1490 768,740	1402-1340	618	510	-
(6)	3500-3330 3320-3080	3530-3270 3260-2820	3145	3480,3420 1335,1270	1681 1655	1612,1605	1509,1490 780,740	1434,1365	621	465	-
(7)	3460-3210 3265-3080	3530-3270 3265-2920	3140	3485,3430 1332,1270	1710 1650	1613 1605	1670,1506 760,700	1425,1335	638	522	-
(8)	3460-3320 3310-3080	3560-3230 3220-2870	3140	3470,3426 1334,1278	1717 1675	1615, 1610	1516,1500 771,740	1422,1402 1265-1340	618	510	-
(9)	3450-3310 3300-3105	3530-3280 3270-2930	3135	3450,3423 1332,1282	1683 1650	1615,1603	1570,1530 765,705	1435,1425 1330,1320	620	505	-
(10)	3450-3360 3500-3100	3510-2280 3270-2850	3160	3416,3350 1335,1272	1718 1655	1620,1607	1504,1474 757,710	1160,1146 1049,690	619	510	-
(11)	3475-3310 3265-3080	3520-3285 3280-2970	3124	3485,3425 1344,1262	1721 1650	1615 1608	1509,1467 765,700	-	610	516	420,405

Table 3, i. Mass spectrum of the ligand [H_4L];**(1)**

m/z	Rel. Int.	Assignments
50	7	NH_4O_2
65	54	C_4H_3N
77	28	C_5H_3N
121	85	C_7H_7NO
223	47	$C_{12}H_{19}N_2O_2$
240	100	$C_{12}H_{20}N_2O_3$
314	8	$C_{17}H_{20}N_3O_3$
390	9	$C_{22}H_{20}N_3O_4$
465	10	$C_{27}H_{20}N_4O_4$
524	18	$C_{29}H_{24}N_4O_6$

Table 3.ii. Mass spectrum of [$(H_4L)(Cu)_2(OAc)_4$].$2H_2O$ complex **(2)**

m/z	Rel. Int.	Assignments
60	92	C_3H_8O
93	22	$C_3H_{11}NO_2$
121	100	$C_5H_{15}NO_2$
185	12	$C_7H_{23}NO_4$
371	19	$C_{15}H_{33}NO_9$
562	14	$C_{26}H_{33}N_3O_{11}$
599	16	$C_{29}H_{34}N_3O_{11}$
661	18	$C_{30}H_{36}N_3O_{14}$
740	18	$C_{31}H_{40}N_3O_{14}Cu$
793	18	$C_{34}H_{41}N_3O_{15}Cu$
959	35	$C_{37}H_{42}N_4O_{17}Cu_2$

Table 3.iii. Mass spectrum of [(H_4L) $(Mn)_2(OAc)_4$].$2H_2O$ complex **(6)**

m/z	Rel. Int.	Assignments
65	30	C_3HN_2
121	100	$C_5H_3N_2O_2$
179	23	$C_7HN_2O_4$
330	14	$C_{14}H_4NO_8$
445	15	$C_{20}H_{15}NO_{10}$
583	18	$C_{24}H_{18}NO_{12}Mn$
649	10	$C_{27}H_{20}N_3O_{14}Mn$

795	12	$C_{33}H_{30}N_3O_{18}Mn$
960	50	$C_{37}H_{46}N_4O_{19}Mn_2$

Thermal analyses (DTA and TGA):

Since the IR spectra indicated the presence of water molecules, thermal analyses (DTA and TGA) were carried out to certain their nature. The thermal curves in the temperature 27-700°C range for complexes (**4**), (**6**), and (**9**) were thermally stable up to 45 °C. Broken of hydrogen bonding occurred as endothermic peak observed within the temperature 45-55 °C as showed in Table 4. Dehydration was characterized by endothermic peaks appeared within the temperature 80-120°C range, corresponding to the loss of hydrated water molecules. The elimination of coordinated water molecules occurred in the 115-130°C range accompanied by endothermic peaks [29, 30]. The thermogram of Co(II) complex **(3)** showed that, the complexes decomposed in six steps. The first occurred at 50°C with no weight loss as endothermic peak, may be due to break of hydrogen bonding. The second step occurred at 75°C with 3.61 % weight loss (Calc. 3.72%) as endothermic peak which could be due to the elimination of two hydrated water molecules. The decomposition step which occurred at 115°C with 2.05% weight loss (Calc. 1.98%) corresponded to the elimination of coordinated water molecules. The endothermic peak observed at 370^{o}c with 27.44% weight loss (Calc. 27.12%), was due to the elimination of four acetate groups. The complex showed an endothermic two peaks observed at 360°C was due its melting point. Finally, exothermic peaks observed at 410, 465, 550, and 630,°C corresponding to oxidative thermal decomposition which proceeded slowly with leaving 2CoO with 23.33% weight loss (Calc. 22.88%)[30]. The thermogram of Mn(II) complex (**6**) showed that, the complex decomposed in six steps. The first occurred at 45°C with no weight loss as endothermic peak, may be due to break of hydrogen bonding. The second step occurred at 85°C with 3.67 % weight loss (Calc. 3.75%) as endothermic peak was due to the elimination of three hydrated water molecules. The decomposition step which occurred at 125°C with 1.83% weight loss (Calc. 1.94%) corresponded to the elimination of two coordinated water molecules. The endothermic peak observed at 240^{o}c with 29.52% weight loss (Calc. 29.94%), was due to the elimination of four acetate groups. The complex showed an endothermic peak observed at 360°C was due its melting point. Finally, exothermic peaks observed at 415,550, 620, and 660°C corresponding to oxidative thermal decomposition which proceeded slowly with leaving 2MnO with 21.18% weight loss (Calc. 21.64%) [31]. The thermogram of Co(II) / Zn(II) complex (**9**) showed that, the complex decomposed in six steps. The first occurred at 55°C with no weight loss as endothermic peak, may be due to break of hydrogen bonding. The second step occurred at 80°C with 3.65 % weight loss (Calc. 3.69%) as endothermic peak which could be due to the elimination of two hydrated water molecules. The decomposition step which occurred at 130°C with 3.80% weight loss (Calc. 3.87%) was due to the elimination of two coordinated water molecules. The endothermic peak observed at 270 with 26.66% weight loss (Calc. 26.63%), could be due to the elimination of four acetate groups. The complex showed an endothermic peak observed at 320°C was due its melting point. Finally, exothermic peaks appeared at 400, 450, 530,610, and 635°C corresponding to oxidative thermal decomposition which proceeds slowly with leaving with of CoO and ZnO 24.05% weight loss (Calc23.99%) [32].The thermal data were presented in Table 4.

Table 4. Thermal data for some metal complexes:

Compound No. Molecular formula	***Temp. (°C)***	***DTA (peak)***		***TGA (Wt. loss %)***		***Assignments***
		Endo	**Exo**	**Calc.**	**Found**	
Complex (4) $[(H_4L)(Co)_2(OAc)_4(H_2O)_2].2H_2O$ $C_{37}H_{40}Co_2N_4O_{16}$	50	Endo	-	-	-	Broken of H-bondings
	75	Endo	-	3.61	3.72	Loss of ($2H_2O$) hydrated water molecules
	115	Endo	-	2.05	1.98	Loss of 2 (H_2O) coordinated water molecules
	370	Endo	-	27.44	27.12	Loss of four coordinated acetate groups
	360	Endo	-	**-**	**-**	Melting point
	410,465, 550,630	-	Exo	23.33	22.88	Decomposition process with the formation of 2CoO
Complex (6) $[(H_4L)\ (Mn)_2(OAc)_4(H_2O)_2].3H_2O$ $C_{37}H_{46}Mn_2N_4O_{19}$	45	Endo	-	-	-	Broken of H-bondings
	85	Endo	-	3.75	3.67	Loss of ($3H_2O$) hydrated water molecules
	125	Endo	-	1.94	1.83	Loss of 2(H_2O) coordinated water molecules
	240	Endo	-	29.94	29.52	Loss of four coordinated acetate groups
	360	Endo	-	**-**	**-**	Melting point
	415,550, 620,660,	-	Exo	21.64	21.18	Decomposition process with the formation of 2MnO
Complex (9) $[(H_4L)(Co)(Zn)(OAc)_4(H_2O)_2].2H_2O$ $C_{37}H_{44}N_4O_{18}CoZn$	55	Endo	-	-	-	Broken of H-bondings
	80	Endo	-	3.67	3.65	Loss of ($2H_2O$) hydrated water molecules
	130	Endo	-	3.90	3.87	Loss of 2 (H_2O) coordinated water molecules
	270	Endo	-	26.66	26.63	Loss of four coordinated acetate groups
	320	Endo	-	**-**	**-**	Melting point
	400,450,530,610, 635	-	Exo	24.04	23.99	Decomposition process with the formation of ZnO and CoO

Magnetic moments:

The magnetic moments of the metal complexes **(2)-(11)** at room temperatures were showed in Table 5. Cu(II) complexes **(2), (8), (10) and (11)** showed values in the 1.72-1.69 B.M, range corresponding to presence of one unpaired electron in an octahedral structure [33, 34]. The low values of complexes were due to spin-spin interactions took place between Cu(II) ions [35]. Co(II) complexes **(4)** and **(9)** showed values 4.28 and 4.6 B.M, indicating high spin octahedral Co(II) complexes [36, 37]. Zn(II) complexes **(5), (8),** and **(9)**, Ag(I) complex **(7)** showed diamagnetic property [38,39]. Ni(II) complex (3), showed values 3.21 B.M, indicating an octahedral Ni(II) complex [40].

Electronic spectra:

The electronic spectral data for the ligand **(1)** and its metal complexes in DMF solution were summarized in Table 5. Ligand **(1)** in DMF solution showed two bands at 295 nm (log€=3.98 x 10^{-3} mol^{-1} cm^{-1}) and 315 nm (log€= 4.25x 10-3 mol^{-1} cm^{-1}) which may be assigned to n→π* and π→π* transitions of the immine group [40]. Copper(II) complexes **(2), (8), (10)** and **(11)** showed bands in the 265-267 and 280-312 nm ranges , these bands were due to intraligand transitions, however, the bands appeared in the 462-478, 570-578 and 602-610 nm ranges, were assigned to O→Cu, charge transfer, $2B_1 \rightarrow 2E$ and $2B_1 \rightarrow 2B_2$ transitions, indicating a distorted octahedral structure[41,42]. However, Co(II) complexes **(4)** and **(9)** showed bands at 270, 293-312, 460, 570 and 615 nm, and 260, 285, 312, 455, 572, and 611nm the first bands were within the ligand and the other bands were assigned to $4T_1g(F) \rightarrow 4T_2g(P)(\nu_3)$, $4T_1g(F) \rightarrow 4A_2g(\nu2)$ and $4T_1g(F)$ $4T_2g(F)(\nu1)$ transitions respectively indicating. However, Ni(II) complex **(3)** showed bands at 268-285, 310-395, 475, 590,617 and 775 nm, the first three bands were within the ligand and the other bands are attributable to O→Ni charge transfer,$3A_2g(F) \rightarrow 3T_1g(P)(\nu3)$, $3A_2g(F) \rightarrow 3T_1g(F)(\nu2)$ and $3A_2g(F) \rightarrow 3T_2g(F)(\nu1)$ transitions respectively, indicating an octahedral Ni(II) geometry. The ν_2/ν_1 ratio was 1.24, which were less than the usual range of 1.5-1.75, indicating a distorted octahedral Ni (II) complex, octahedral structure[43]. Zinc(II) complexes **(5), (8),** and **(9)**, Silver**(I)** complex **(7),** showed bands were due to intraligand transitions [41, 47].

Table 5. The electronic absorption spectral bands (nm) and magnetic moments (B.M.) for the ligand $[H_4L]$ (1), and its complexes

Electron spin resonance (ESR):

No.	**λ_{max} (nm)**	**μ_{eff} in B.M.**	**ν_2/ν_1**
(1)	295 nm (log ε =3.8×10^{-3})mol^{-1} cm^{-1}, 315 nm (log ε =4.25×10^{-3}) mol^{-1} cm^{-1}	-	-
(2)	267,280,305,470,575,607	1.69	
(3)	268,285,310, 475,590,617,776	3.21	1.24
(4)	270,290,312,460,570,615	4.28	-
(5)	268,283,310	Diamagnetic	
(6)	265,280,307,462,568,612	5.61	
(7)	267,285,310	Diamagnetic	
(8)	265,283,310,460,570,610	1.71	-
(9)	260,285,312,455,572,611	4.61	-
(10)	265,280,305,478,575,602	1.72	
(11)	266,282,307,462,578,605	1.70	

The ESR spectral data for complexes **(2), (4), (6), (8)** and **(10)** were presented in Table 6. The spectra of Cu(II) complexes **(2)** and **(11)** were characteristic of species d^9, configuration having axial type of a $d(x^2-y^2)$ ground state which is the most common for Cu(II) complexes[47,48]. The complexes showed $g_{\|}>g_{\perp}>2.0023$, indicating octahedral geometry around Cu(II) ion. The g-values are related by the expression $G = (g_{\|}-2)/ (g_{\perp} -2)$, where (G) exchange coupling interaction parameter (G). If G<4.0, a significant exchange coupling is present, whereas if G value > 4.0, local tetragonal axes are aligned parallel or only slightly misaligned. Complexes **(2)** and **(11)**

showed 2.33 and 2.75 values indicating spin-exchange interactions took place between Cu(II) ions. This phenomenon is further confirmed by the magnetic moments values (1.69 and 1.70 B.M.). The g||/A|| value is also considered as a diagnostic term for stereochemistry, the g||/A|| values were 210 and 175.8 which were expected for distorted octahedral complexes. The g-values of Cu(II) complexes with a $2B_1g$ ground state ($g_{||}>g_{\perp}$) may be expressed by K_{11}^2 [47].

$$g_{||} = 2.002 - (8K^2_{||}\lambda^\circ/\Delta Exy) \quad (1)$$

$$g_{\perp} = 2.002 - (2K_{2\perp}\lambda^\circ/\Delta Exz) \quad (2)$$

Where $k_{||}$ and $k_{\perp}$ are the parallel and perpendicular components respectively of the orbital reduction factor (K), λ° is the spin-orbit coupling constant for the free copper, ΔExy and ΔExz are the electron transition energies of $2B_1g \rightarrow 2B_2g$ and $2B_1g \rightarrow 2Eg$. From the above relations, the orbital reduction factors ($K_{||}$, $K_{\perp}$, K), which are measure terms for covalency [47], can be calculated. For an ionic environment, K=1; while for a covalent environment, K<1. The lower the value of K, the greater is the covalency.

$$K_{\perp}^2 = (g_{\perp} - 2.002)\,\Delta Exz\,/2\lambda o \quad (3)$$

$$K^2_{||} = (g_{||} - 2.002)\,\Delta Exy\,/8\lambda o \quad (4)$$

$$K^2 = (K^2_{||} + 2K_{\perp}^2)/3 \quad (5)$$

K values (Table 6), for the Cu(II) complexes **(2)** and **(11)** were indicating for a covalent bond character[47,48]. Kivelson and Neiman noted that, for ionic environment $g_{||} \geq 2.3$ and for a covalent environment g||<2.357. Theoretical work by Smith [48] seems to confirm this view. The g-values reported here (Table 6) showed considerable covalent bond character [48]. Also, the in-plane σ-covalency parameter, α2(Cu) was calculated by

$$\alpha^2(Cu) = (A||/0.036)+(g||-2.002)+3/7(g_{\perp} -2.002)+0.04 \quad (6)$$

The calculated values (Table 6) suggested a covalent bonding. The in-plane and out of- plane π- bonding coefficients β^2_1 and β^2 respectively, are dependent upon the values of ΔExy and ΔExz in the following equations[49].

$$\alpha^2\beta^2 = (g_{\perp} - 2.002)\,\Delta Exy/2\lambda o \quad (7)$$

$$\alpha^2\beta_1^2 = (g|| - 2.002)\,\Delta Exz/8\lambda o \quad (8)$$

In this work, the complexes **(2),** and **(11)** showed β_1^2 values 0.60, and 0.36 indicating a covalency in the in-plane π-bonding[50]. β^2 value for complexes **(2),** and **(11)** showed 0.83 and 0.92 indicating covalent character of the out-of-plane[50]. It is possible to calculate approximate orbital populations ford orbitals[60] by

$$A|| = A_{iso} - 2B[1 \pm (7/4)\,\Delta g||]\ \Delta g_{||} = g_{||} - ge \quad (9)$$

$$a^2d = 2B/\,2B^\circ \quad (10)$$

Where A° and 2B° is the calculated dipolar coupling for unit occupancy of d orbital respectively. When the data are analyzed, the components of the ^{60}Cu hyperfine coupling were considered with all the sign combinations. The only physically meaningful results are found when $A_{||}$ and $A_{\perp}$ were negative. The

resulting isotropic coupling constant was negative and the parallel component of the dipolar coupling 2B are negative (-175, 0 and -222.2 G). These results can only occur for an orbital involving the (dx^2-y^2) atomic orbital on copper. The value for 2B is quite normal for Cu(Il) complexes. The $|A_{iso}|$ value was relatively small. The 2B value divided by 2Bo (The calculated dipolar coupling for unit occupancy of dx2-y2 (235.11 G), using equation **(10)** suggested all orbital population are 74.3 and 94.5% d-orbital spin density, clearly the orbital of the unpaired electron is dx^2-y^2. However, Co(II) complex **(4)**, Mn(II) complex **(6)**,[Cu(II)/Zn(II)]complex **(8),**and Cu(II)complex **(10),** showed isotropic values 2.04,2.03, 2.07, and 2.05 respectively indicating octahedral structure with covalent bond character[51].

No.	$g_{\parallel}$	$g_{\perp}$	g_{iso} [a]	$A_{\parallel}$ (G)	$A_{\perp}$ (G)	A_{iso} [b] (G)	G [c]	ΔE_{xy}	ΔE_{xz}	$K_{\perp}^2$	$K_{\parallel}^2$	K	K^2	$g_{\parallel}/A_{\parallel}$	α^2	$ß^2$	$ß_1^2$	2 ß	a_d^2 (%)
(2)	2.10	2.03	2.05	1.05	7.5	40	3.33	17534	21052	0.63	0.26	0.57	0.33	210	0.43	0.83	0.60	175	74.3
(4)	-	-	2.04	-	-	-	-	-	-	-	-	-	-	-	-	-	-	-	-
(6)	-	-	2.07	-	-	-	-	-	-	-	-	-	-	-	-	-	-	-	-
(10)	-	-	2.05	-	-	-	-	-	-	-	-	-	-	-	-	-	-	-	-
(11)	2.11	2.04	2.06	130	10	50	2.75	18868	20202	0.45	0.31	0.36	0.4	175.8	0.49	0.92	0.63	222.2	94.5

Table (6): ESR data for the metal complexes:

$g_{iso}=(2g_{\perp}+g_{\parallel})/3$

Transmission electron microscopic characterization (TEM)

The average diameter of the complexes particles under study was found to be 7.18 -82.4 nm as showed in figures **(3)** and **(4)** respectively. The particles are present in Nano-Size form (1-100 nm). The complexes showed enhanced size dependent properties Compared with larger particles of the same type of complexes such as increased bioavailability, dose proportionality, decreased toxicity, smaller dosage form (smaller tablets), stable dosage forms of drugs which are either unstable or have Unacceptably low bioavailability in non- nano particulate dosage forms, increased active agent surface area results in a faster dissolution of The active agent in an aqueous environment such as human body, faster dissolution, with greater bioavailability, smaller drug doses, less toxicity and reduction in fed/fasted variability[52]. The TEM images for Cu(II) complex **(2)** and Cu(II)/Zn complex **(8)** were showed in Figures (3)- (4) respectively.

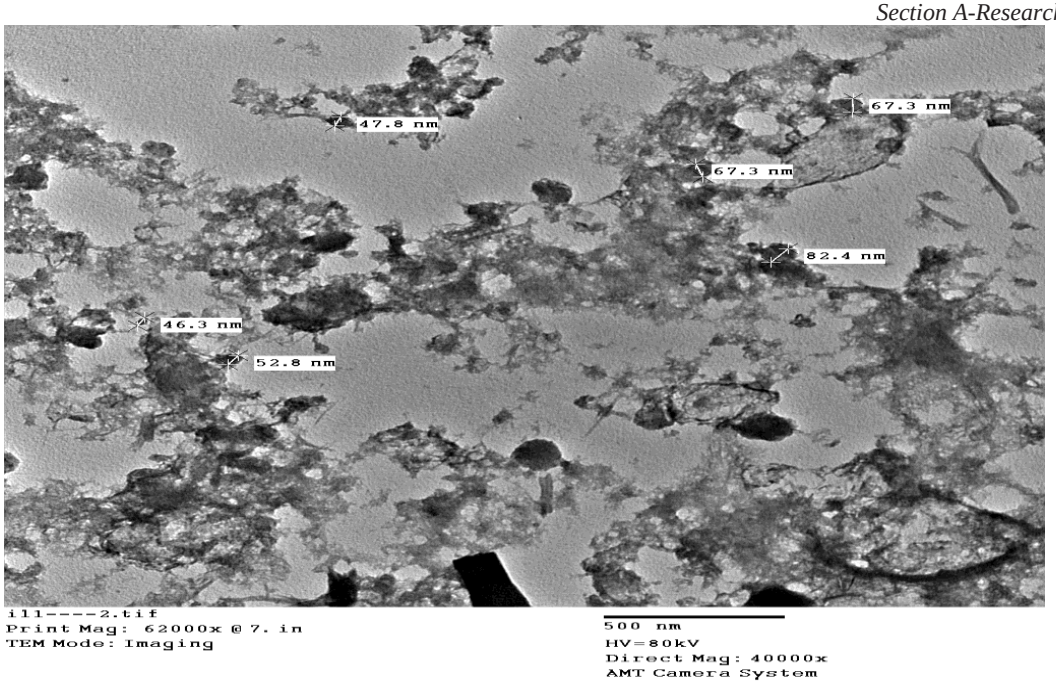

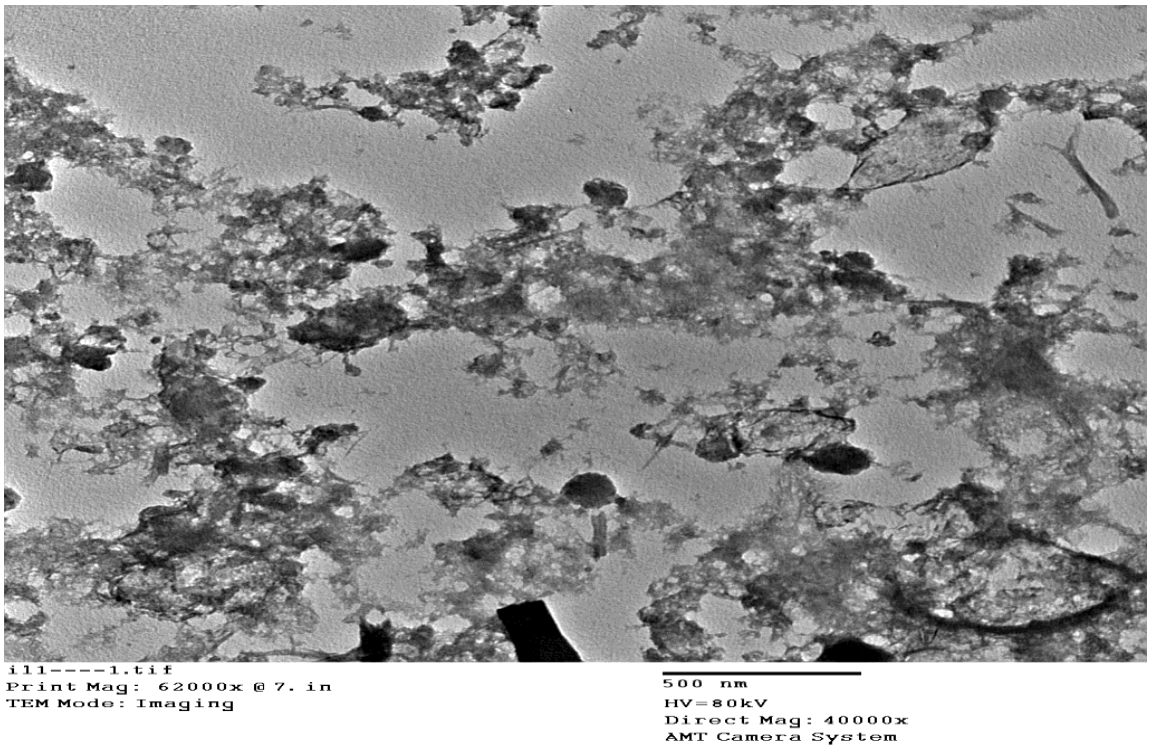

Fig (3): TEM image for Cu(II) complex **(2)** nanoparticles

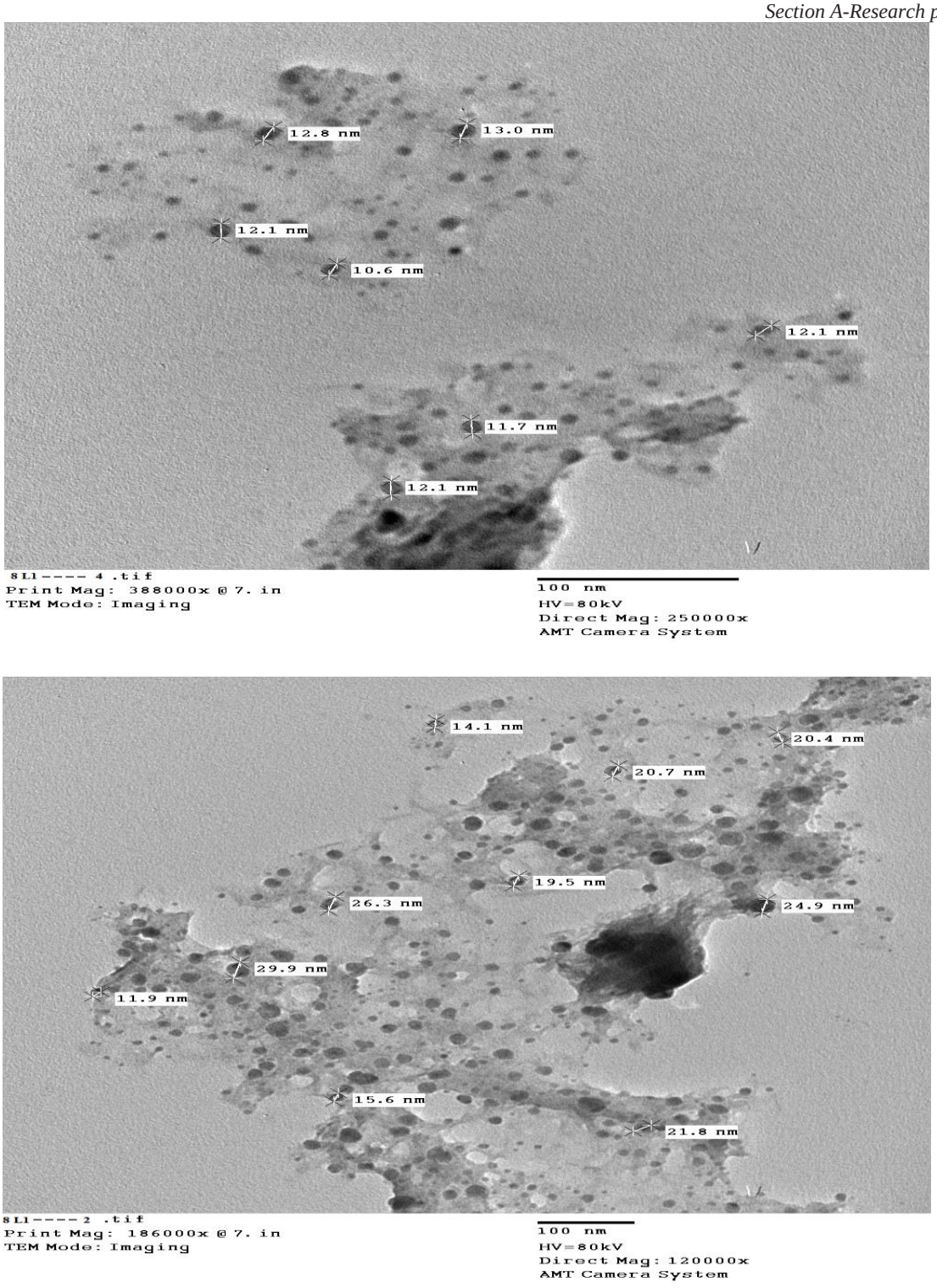

Fig (4): TEM image for Cu(II)/Zn complex **(8)** nanoparticles

Chemotherapeutic studies:

The biological activity of the ligand **(1)** and its metal complexes **(2)** and **(8)** were evaluated against MCF-7 cell lines figures (5-7). In this study, we try to know the chemotherapeutic activity of the tested complexes by comparing them with the standard drug (Cisplatin). It seems that, changing the anion, coordination sites and the nature of the metal ion has effect on the biological behavior by altering the binding ability of DNA [50-54]. Gaetke and Chow had reported that, metal has been suggested to facilitate oxidative tissue injury through a free-radical mediated pathway analogous to the Fenton reaction. It was showed that, the Cu(I) complexes are able to form GSSG (Glutathione disulfide) via the following reactions:

$$[Cu(I)\ (ligand)] + GSH \rightarrow [Cu(I)\ (GS)] + ligand + H^{+} \quad (11)$$

$$[Cu(I)\ (GS)] + GS+ [Cu(II) + GSSG \quad (12)$$

These reactions lead to depletion of intracellular GSH pools, which has been frequently observed in cells after treatment with diverse Cu compounds [56-58]. In the presence of H_2O_2, the DNA-bound Cu(II) complex is oxidized to form presumably Cu(II) (oxo/ hydroxo) species [52-.57], thus, the reaction of Cu(II) complex with nucleic acid is occurred via Cu-oxo/ hydroxo intermediate. Cu(II) complexes are well known for their redox activity, which seems to be responsible for biological activities [53]. The redox cycling of Cu complexes is based on the reduction of Cu(II) to Cu(I) by intracellular thiols such as GSH (glutathione, nonenzymatic antioxidant under oxygen-contaning conditions" reaction pathway for [Cu(II) (ligand)] complexes was given in equations (13 - 15). Briefly, Cu(II) schematically, the underlying complexes rapidly form adducts with GSH[53], leading to Cu(I) complexes and GS+. In the presence of oxygen, this Cu(I) complex is able to generate a superoxide anion, which can induce ROS via a fentonlike reaction:

$$[Cu(II)\ (ligand)] + GSH \rightarrow [(GS)\ Cu(II)\ (ligand)] + H^{+} \quad (13)$$

$$[(GS)\ Cu(II)\ (ligand)] \rightarrow [GS^{*} + [Cu(I)\ (ligand)] \quad (14)$$

$$[Cu(I)\ (ligand)] + O2 \rightarrow O_2 + [Cu(II)\ (ligand)] \quad (15)$$

The treatment of the different complexes in DMSO showed similar effect in the tumoral cell line used as it was previously reported [54]. The solvent dimethyl sulphoxide (DMSO) showed no effect in cell growth. The ligand **(1)** showed a weak inhibition effect at ranges of concentrations used, however, the complexes showed better effect against MCF-7 cell lines. The data obtained indicated the surviving fraction ratio against MCF-7 tumor increasing with the decrease of the concentration in the range of the tested concentrations [55]. Cytotoxicity results indicated that the tested complexes **(2),** and **(8)** demonstrated potent. Copper (II) complex **(2)** showed the cytotoxicity effect against cell line with IC_{50} value of 12.8 μM, and then complex **(8)** with IC_{50} value **0.8** μM.IC_{50} of complex **(8)** comparing with standard drug (Cisplatin) which is 5.69 at all concentrations complex **(8)** may be showed a good drug for treatment of MCF-7 cell lines .This can be explained as Cu (II) ion bonded to DNA. It observed that, changing the anion and the nature of the metal ion has effect on the biological behavior, due to alter Binding ability of DNA binding, so testing of different complexes is very interesting from this point of view. Chemotherapeutic activity of the complexes may be attributed to the central metal atom which was explained by Tweedy's chelation theory [56, 57]. Also, the positive charge of the metal increases the acidity of coordinated ligand that bears protons, leading to stronger hydrogen bonds which enhance the biological activity [58, 59]. The cytotoxic effect of the ligand and some of its metal complexes against MCF-7 cell lines were presented in table (7).

The histograms of standard drug (cisplatinss) ,complexes **(2)** and **(8)** at different concentrations were shown in figures (5)-(7) respectively

Table 7: Cytotoxic effect of the ligand and some of its complexes against MCF-7 cell line

concentration	Order of cytotoxic effect of studied complex against MCF-7 cell line
500 µg/ml	**(8)**> cisplatin> **(2)**> ligand
250 µg/ml	**(8)**> cisplatin> **(2)**> ligand
62.5 µg/ml	**(8)**> cisplatin> **(2)**> ligand
15.6 µg/ml	**(8)**> cisplatin> **(2)**> ligand
3.9 µg/ml	**(8)**> cisplatin> **(2)**> ligand
1.0 µg/ml	**(8)**> cisplatin> **(2)**> ligand

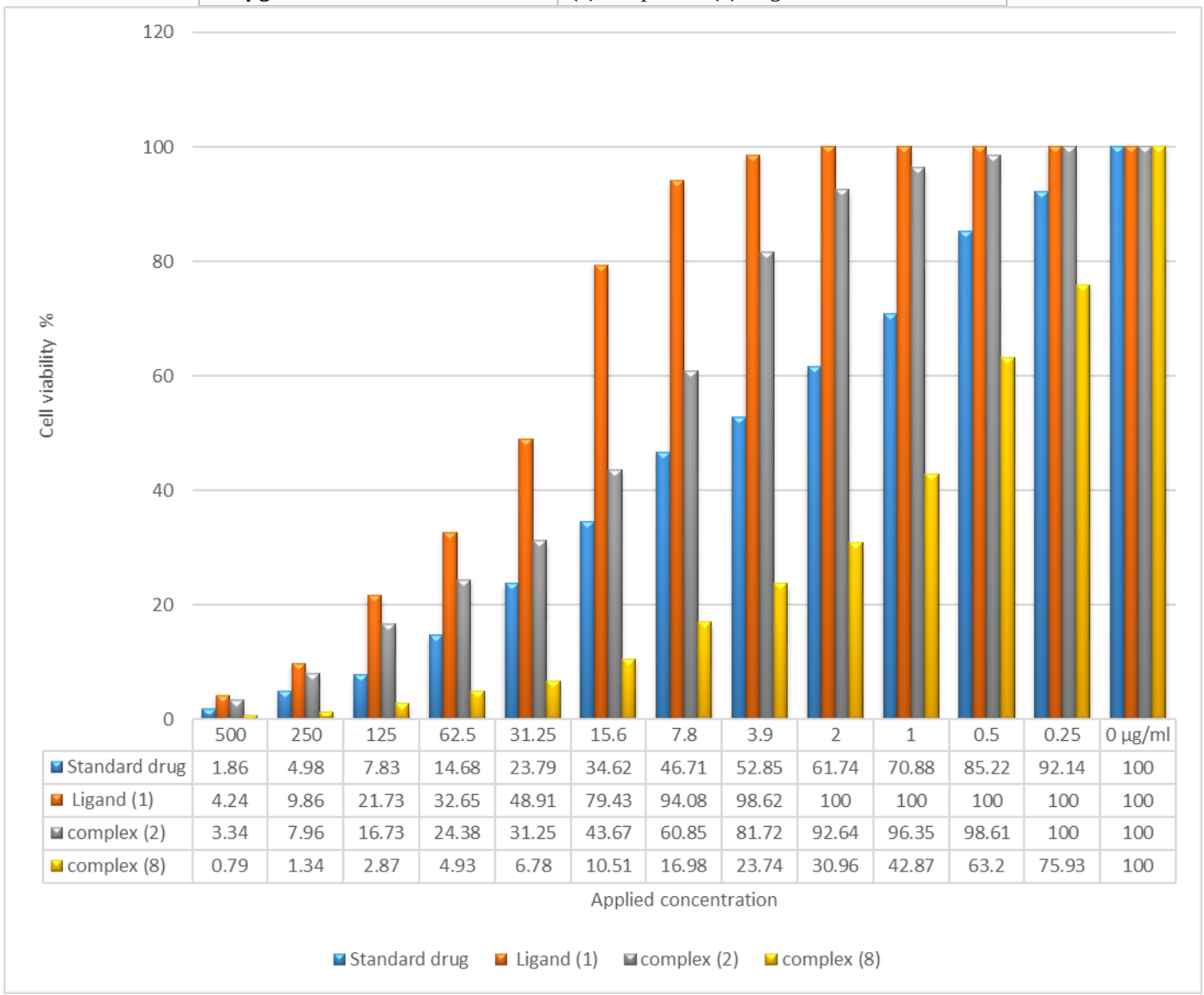

	500	250	125	62.5	31.25	15.6	7.8	3.9	2	1	0.5	0.25	0 µg/ml
Standard drug	1.86	4.98	7.83	14.68	23.79	34.62	46.71	52.85	61.74	70.88	85.22	92.14	100
Ligand (1)	4.24	9.86	21.73	32.65	48.91	79.43	94.08	98.62	100	100	100	100	100
complex (2)	3.34	7.96	16.73	24.38	31.25	43.67	60.85	81.72	92.64	96.35	98.61	100	100
complex (8)	0.79	1.34	2.87	4.93	6.78	10.51	16.98	23.74	30.96	42.87	63.2	75.93	100

Fig (5): Evaluation of cytotoxicity of metal complexes against human MCF-7 cell line

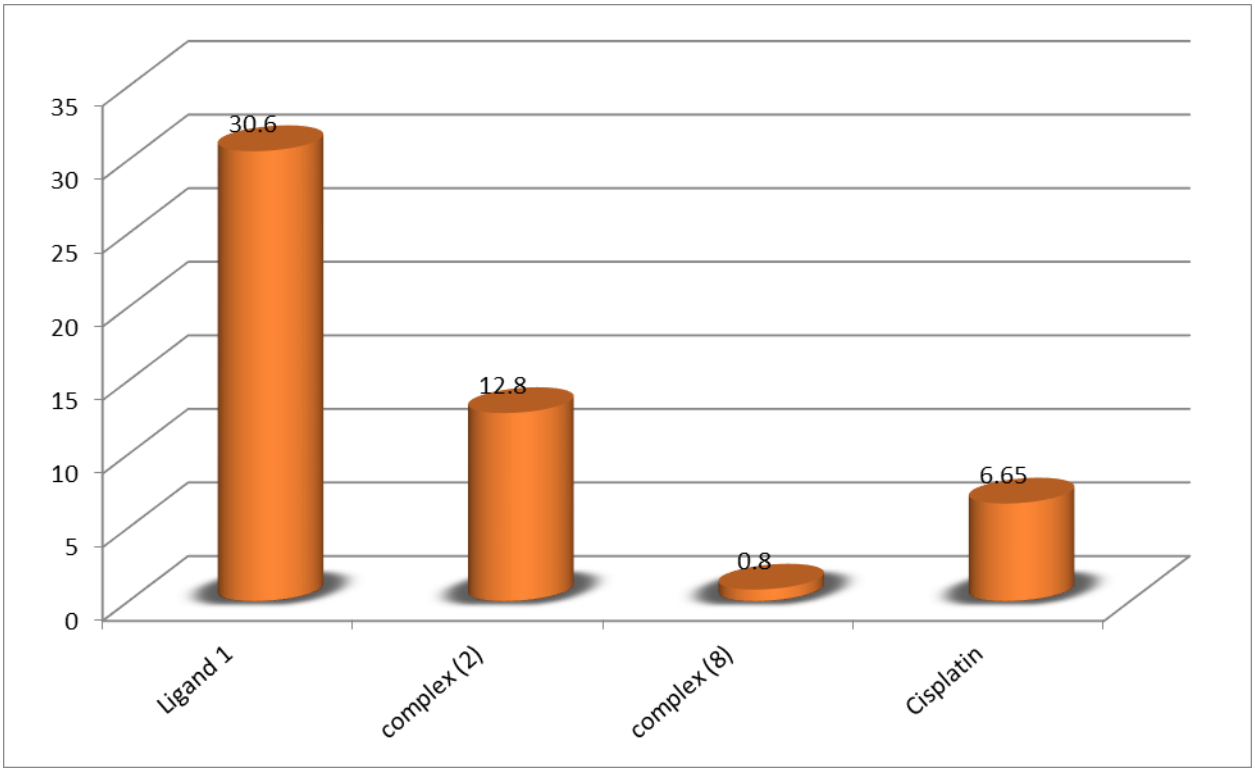

Fig (6): IC_{50} values of the ligand, and some of its metal complexes against human MCF-7 cell lines

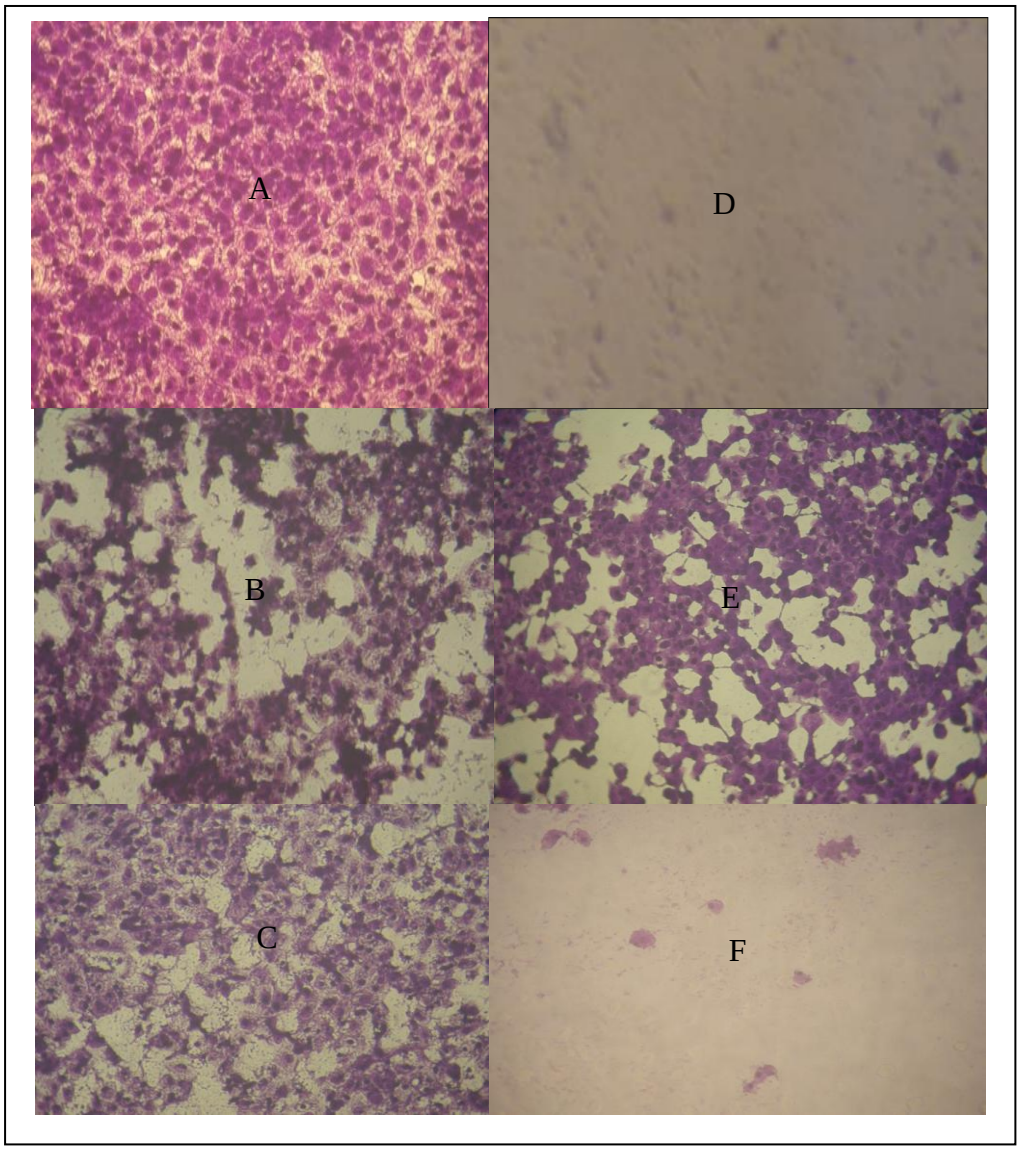

Fig (7): Histogram show MCF-7 cells; **A**- non-treated MCF-7 cells ,**B**- MCF-7 cell line treated with complex **(2)** at 0.5 µg/ml, **C**- MCF-7 cell line treated with complex **(2)** at 100 µg/ml, **D**- MCF-7 cell line treated with complex **(8)** at 0.5 µg/ml, **E**- MCF-7 cell line treated with complex **(8)** at 100 µg/ml and **F**- MCF-7 cell line treated with complex **(8)** at 500 µg/ml

CONCLUSION

In the present study, new metal complexes of the ligand were prepared. Structural and spectroscopic properties revealed that, the ligand adopted a hexadentate ligand fashion; on the other hand, the metal complexes adopted a distorted octahedral geometry around metal ions. All the complexes were non-electrolytic in nature as suggested by molar conductance measurements. The ligand coordinated to the central metal ion forming six membered rings including the metal ions. The antitumor activities against (MCF-7 cell lines) of the ligand as well as some of its metal complexes were assessed that, the toxicity of both ligand and metal complexes was found to be concentration dependent, the cell viability decreased with increasing the concentration of complexes.

ACKNOWLEDGMENT

We thank the laboratory of materials and renewable energy and the central laboratory, Faculty of Science, Menofia University for doing UV measurements.

FUNDING:

The author(s) received no financialsupport for the research or authorship.

CONFLICTS OF INTEREST:

The authors have declared no conflict of interest.

REFERENCES

1. El-Tabl, A.S., Abd-Elzaher F.A., Shakdofa M M., E.Rasras M.M., Anas J.., Synthesis, physicochemical studies and biological evaluation of unimetallic and heterobimetallic complexes of hexadentatedihydrazone ligands.Beni-Suef University Journal of Basic and Applied Sciences,. 6(1): p. 24-32(2017).
2. El-Tabl, A.S., et al., Synthesis, structural characterization, electrochemical and biological studies on divalent metal chelates of a new ligand derived from pharmaceutical preservative, dehydroacetic acid, with 1, 4-diaminobenzene. Arabian Journal of Chemistry,. 10: p. S3816-S3825(2017).
3. El-Tabl, A.S., Abd-El Wahed M .M., and Abu-Setta M.H.H., metallo-bioactive compounds as potential novel anticancer therapy. Journal of Chemistry and Chemical Sciences (2015).
4. El-Tabl A, S,., et al., Synthesis, Structural Characterization and Study of Some New Antimicrobial Action of Metal Complexes of (E)-N', N''-bis ((Z)-4-fluorobenzylidene)-2- (naphthalen-1-yloxy) acetohydrazono-hydrazide Schiff Base. Journal of Chemistry and Chemical Sciences,. Vol.6 (6): p. 513-536(2016).
5. El-Tabl A. S, Abd-El Wahed M.M., and Hashim S.M.F., Metal Chelates as Antitumor Agents: Synthesis, Spectroscopic Characterization and Cytotoxic Action of Metal Chelates of New Dioxime Ligand. Journal of Chemistry and ChemicalSciences,.Vol.8(8),:p. 1026-1047(2018).
6. El-Tabl A. S, Abd-El Wahed M.M., and El-Saied S.A.-E.R.,Design, Spectroscopic Characterization and Antitumor Action of Synthetic Metal Complexes of Novel BenzohydrazideOxime. Journal of Chemistry and Chemical Sciences,. Vol.8(8),: p. 1048- 1072(2018).
7. EL-Tabl A. S.; Wassel M. A. and Arafa M. M., Preparation and investigation of fulvic acid and its metal derivative complexes SScientific and Engineering Research,:p1663-1679(2017).
8. Wassel M.A., EL-Tabl A.S., Arafa M. M. and Alhalib A. A., synthesis, analytical and physical data of ligand (H6L) and its metal, International Journal of Scientific and Engineering Research,:p 1122-1135(2017)

9. EL-Tabl A.S.; Wassel M. A., Arafa M.M., Alhalib A.A. and Wassel A., Thermal analysis (DTA and TGA) of ligand (H6L) and its metal complexes Co(II), Fe(II), Cu(II) AND Ni(II). , International Journal of Scientific and Engineering Research,:p 2044-2052(2017).

10. EL-Tabl A.S.; Abd El-wahed M. M. and khalefa S.M., Synthesis and spectroscopic characterization of bioactive compounds derived from glutamic acid; study of their antimicrobial and antiproliferative properties , International Journal of Scientific and Engineering Research,:p 2114-2126(2018).

11. EL-Tabl A.S.; Abd El-wahed M.M. and El-Saied S.A, Design , Spectroscopic characterization and antitumor action of synthetic metal complexes of novel benzohydrazide oxime, Journal of Chemistry and Chemical Sciences (2019)

12. El-Tabl A S., Abd-El Wahed M.M., Shakdofa M M. Herisha B.M, Metal complexes of a new asymmetric hydrazonic ligand synthesis, characterization and microbicide Activities International Journal of Scientific and Engineering Research, Volume 10, Issue 2, (2019)

13. El-Tabl A S., Abd-El Wahed M.M., Nabawy A A, Faheem S M, Preparation, Spectroscopy Characterization and Anticancer Activity of New Polyhydroxy Ligand and its Metal Complexes, Journal of Chemistry and Chemical Sciences, Vol.10(5), 230-252,(2020).

14. El-Tabl A S., Abd-El Wahed M.M., El-Basyouny M M., and Faheem S.M, Preparation, Spectroscopic Characterization and Antitumor Activity of New Metal ComplexesofSodium4,4'-((2E,2'E)-2,2'-((4,6-dihydroxy-1,3-phenylene)bis(ethan-1-yl-1ylidene))bis(hydrazinecarbonyl))diphenolate hydrate,Journal of Chemistry andChemical Sciences,Vol.10(5), 177-200, (2020).

15. El-Tabl A S, Gharieb M M, Hemida H S and Faheem S M, Synthesis, Structural Characterization and Antimicrobial Study on Metal Complexes of New Bioactive Ligand with Terminal Wings, Journal of Chemistry and Chemical Sciences, Vol.10(2), 65-85, (2020)

16. El-Tabl A S., Abd El-wahed M M., Sayed Ahmed R A and Sarhan K S., Synthesis and Structural Characterization of New and Exciting NP Complexes-based Paracetamol Moiety with Antimicrobial Activity, Journal of Chemistry and Chemical Sciences, 34 Vol.10(1), 32-64, (2020).

17. El-Tabl A S, Abd El-Wahed M M, Abo El-Azm M I, and Faheem S M, Newly Designed Metal-based Complexes and their Cytotoxic Effect on Hepatocellular Carcinoma, Synthesis and Spectroscopic Studies, Journal of Chemistry and Chemical Sciences, Vol.10(1), 10-31, (2020).

18. El-Tabl A S., Zawam S A, Sarhan K S, Innovating new methods for wastewater treatment in El-Dakhla Oasis in Upper Egypt from

chemical and biological pollutants using modified Down flow Hanging Sponge (DHS) reactor in presence of new environmental friendl chelator, Egyptian Journal of Chemistry, Accepted, (2020).

19. El-Tabl A S, Abd El-Wahed M M, El Assaly M M.and Ashour A M., Nanoorganometallic complexes as therapeutic platforms against breast cancer cell lines; (in vitro study), Egyptian Journal of Chemistry, volume 64, issue3, (2021).

20. El-Tabl A S, Abd El-Wahed M M, Wahed, Abd-Elwareth M M, Faheem S M, Nano metal complexes in cancer therapy, preparation, spectroscopic, characterization and anti-breast cancer activity of new metal complexes of alanine Schiff-base, Egyptian Journal of Chemistry, Accepted, (2021).

21. Lever and Philip, A. B. Inorganic electronic spectroscopyAmsterdam: Elsevier, (1968).

22. Bosch, F. and L. Rosich, The contributions of Paul Ehrlich to pharmacology: a tribute on the occasion of the centenary of his Nobel Prize. Pharmacology, 2008. 82(3): p. 171-179.

23. Abdou, S., et al. "Cytotoxicity and antitumor activity of organometallic copper (II) Nano particles in a chemically induced hepatocellular carcinoma rat model." (2022).

24. Vogel, A. ELBS, Vogel's textbook of quantitative inorganic analysis, including elementary instrumental analysis 4th. Edn. London and New York.

25. Naskar, S., {Naskar, Sumita and Naskar, Subhendu and Mondal, Satyajit and Majhi, Paresh Kumar and Drew, Mike GB and Chattopadhyay, Shyamal Kumar, Synthesis and spectroscopic properties of cobalt (III) complexes of some aroyl hydrazones: X-ray crystal structures of one cobalt (III) complex and two aroyl hydrazone ligands. Inorganica Chimica Acta, 371(1): p. 100-106.(2011)

26. Bakheit and Satyanarayana.S, Vitamin B12 Model complexes: synthesis and characterization of thiocyanato cobaloximes and thiocyanato bridged dicobaloximes of o- donor ligands: DNA Binding and antimicrobial activity J. Korean Chem. Soc. 6(54): p.687.(2010)35

27. El-Tabl A S. et al. Synthesis and physico-chemical studies on cobalt (II), nickel (II) and copper (II) complexes of benzidine diacetyloxime. Transition Metal Chemistry. 27(2): p. 166-170.(2002)

28. Aly, M., Baghlaf. A and Ganji.N.Linkage isomerism of the oximato group: the characterization of some mono-and binuclear square planar nickel (II) complexes of vicinal oxime-imine ligands. Polyhedron. 4(7): p. 1301-1309.(1985)

29. Nakamoto, K. Infrared and Raman spectra of inorganic and coordination compounds.: Wiley Online Library.(1978).

30. El-Tabl A S., Abd-El Wahed M M.; Whaba M,.and Shebl M, Synthesis, spectroscopic characterization and biological activity of the metal complexes of the Schiff base derived from phenylaminoacetohydrazide and dibenzoylmethane. Spectrochimica Acta Part A: Molecular and Biomolecular Spectroscopy,. 71(1): p.90-99.(2014)

31. El-Tabl A S., A.S.Novel N, N-diacetyloximo-1, 3-phenylenediamine copper (II) complexes. Transition Metal Chemistry,. 22(4): p. 400-405 (1997).

32. Aly, M.M. and Imam,S.M. Site occupancy and reactivity of nickel (II) and palladium (II) coordination compounds of vicinal oxime-imine ligands: an interpretation to the phenomenon of chelate isomerism in the same molecule. Polyhedron, 13(12): p. 1907-1916 (1994).

33. El-Reash, G.M.A., K.M. Ibrahim, and Bekheit,M.M. Ligational behaviour of biacetylmonoxime nicotinoyl hydrazone (H2BMNH) towards transition metal ions. Transition Metal Chemistry, 15(2): p. 148-151 (1990)

34. Chaudhary N K and Mishra P. Metal Complexes of Novel Schiff Base Based on Penicillin: Characterization, Molecular Modeling, and Antibacterial Activity Study. Bioinorganic Chemistry and Applications., ID 6927675(2017).

35. Lever, A., Electronic spectra of some transition metal complexes: Derivation of Dq and B. Journal of Chemical Education, 45(11): p. 711 (1968).

36. Aslan, H.G., Özcan, S. and Karacan,N. Synthesis, characterization and antimicrobial activity of salicylaldehyde benzenesulfonyl hydrazone (< i> Hsalbsmh and its Nickel (II), Palladium (II), Platinum (II), Copper (II), Cobalt (II) complexes. Inorganic Chemistry Communications,. 14(9): p. 1550-1553 (2011).

37. Mohamed, G.G., Omar,M. and Hindy, A.M. Synthesis, characterization and biological activity of some transition metals with Schiff base derived from 2-thiophene carboxaldehyde and aminobenzoic acid. Spectrochimica Acta Part A: Molecular and Biomolecular Spectroscopy,. 62(4): p. 1140-1150 (2005)36

38. Geary, W.J., The use of conductivity measurements in organic solvents for the characterisation of coordination compounds. Coordination Chemistry Reviews,. 7(1): p. 81-122.(1971).

39. El-Tabl AS., Abd-El Wahed M M.; Whaba M, Synthesis, spectroscopic investigation and biological activity of metal (II) complexes with N2O4 ligands. Journal of Chemical Research,. 2009(9): p. 582-587.(2009).

40. Surati, K.R. and Thaker,B. Synthesis, spectral, crystallography and thermal investigations of novel Schiff base complexes of manganese (III) derived from heterocyclic β-diketone with aromatic and aliphatic diamine. Spectrochimica Acta Part A: Molecular and Biomolecular Spectroscopy,. 75(1): p. 235-242.(2010).

41. Surati, K.R., Synthesis, spectroscopy and biological investigations of manganese (III) Schiff base complexes derived from heterocyclic β-diketone with various primary amine and 2, 2′-bipyridyl. Spectrochimica Acta Part A: Molecular and Biomolecular Spectroscopy,. 79(1): p. 272-277.(2011)

42. Figgis, B.N., Introduction to Ligand Fields., Interscience Publishers.(1966).

43. Akbar A, M., Ali, Akbar M and Mirza, Aminul Huq and Yee, Chiam Yin and Rahgeni, Hayatti and Bernhardt, Paul V}, Mixed-ligand ternary complexes of potentially pentadentate but functionally tridentate Schiff base chelates. Polyhedron,. 30(3): p. 542-548 (2011).

44. El-Tabl AS., Abd-El Wahed M M.; Whaba M, Synthesis of novel metal complexes with isonicotinoyl hydrazide and their antibacterial activity. Journal of Chemical Research,. 34(2): p. 88-91 (2010).

45. Karlin, K.D. and Zubieta,J. Copper Coordination Chemistry: Biochemical and inorganic Perspectives.: AdeninePress (1983).

46. Hathaway, B. and Billing,D. The electronic properties and stereochemistry of mono-nuclear complexes of the copper (II) ion. Coordination Chemistry Reviews,. 5(2): p. 143-207 (1970).

47. Al-Hakimi,A.N. El-Tabl,A.S. and Shakdofa,M.M. Coordination and biological behaviour of 2-(p-toluidin) -N'-(3-oxo-1,3 -diphenyl propylidene)acetohydrazide and its metal complexes. Journal of Chemical Research,12. (2009).

48. Suvarapu L N, Young K S, Okbaek S and Reddy V A., Review on Analytical and Biological applications of Hydrazones and their Metal Complexes. Journal of Chemistry and Chemical Sciences., 9(3), 1288-1304.(2012).

49. Smith, D., Chlorocuprates (II). Coordination Chemistry Reviews,. 21(2): p. 93-158 (1976). 3750. Kivelson, D. and R. Neiman, ESR studies on the bonding in copper complexes. The Journal of Chemical Physics,. 35(1): p. 149-155 (1961).

50. El-Tabl A S.; Whaba M. EL-assaly A. S., and Saad A. L.. Sugar Hydrazone Complexes; Synthesis, Spectroscopic Characterization and Antitumor Activity. Journal of Advances in Chemistry,. 9(1): p. 1837-1860 (2014).

51. Surati, K. R.and Thaker, B. Spectrochimica Acta Part A: Molecular and Biomolecular Spectroscopy., 75, 235-242 (2010).

52. El-Tabl A, S., Abd-El Wahed M M., and Ashour A M.. "Metallo-organic Copper (II) Complex in Nano Size as a New Smart Therapeutic Bomb for Hepatocellular Carcinoma." Journal of Chemistry and Chemical Sciences 9(1): p.33-44 (2019)

53. Z. Wail Al, "Synthesis of macrocyclic Schiffbases based on pyridine-2, 6-dicarbohydrazide and their use in metal cations extraction, Organic Chemistry Current Research, 2012.

54. Avaji P. G., Patil S. A., and Badami P. S., Synthesis, spectral, thermal, solid-state DC electrical conductivity and biological studies of Co(II) complexes with Schiffbases derived from 3-substituted-4-amino-5-hydrazino-1, 2, 4-triazole and substituted salicylaldehydes, Transition Metal Chemistry, vol. 33, pp. 275-283, (2008).

55. Opletalová V., Kalinowski D. S., Vejsov M., Kune J. ., Pour M., Jamp lek J., et al., Identification and characterization of thiosemicarbazones with antifungal and antitumor effects: cellular iron chelation mediating cytotoxic activity, Chemical Research in Toxicology, vol. 21, pp. 1878-1889, (2008).

56. El-Tabl A S., Shakdofa M. M., and El-Seidy A., Synthesis, Characterization and ESR Studies of New Copper(II) Complexes of Vicinal Oxime Ligands, Journal of the Korean Chemical Society, vol. 55, pp. 603-611, (2011).

57. Lima L. M., Frattani F. S., dos Santos J. L., Castro H. C., Fraga C. A. M., Zingali R. B., et al., Synthesis and anti-platelet activity of novel arylsulfonate–acylhydrazone derivatives, designed as antithrombotic candidates, European Journal of Medicinal Chemistry, vol. 43, pp. 348-356, (2008).

58. Bernhardt P. V., Mattsson J., and Richardson D. R., Complexes of cytotoxic chelators from the dipyridyl ketone isonicotinoyl hydrazone analogues, Inorganic Chemistry, vol. [232] D. A. Green, W. E. Antholine, S. J. Wong, D. R. Richardson, and C. R. Chitambar, "Inhibition of Malignant Cell Growth by 311, a Novel Iron Chelator of the Pyridoxal Isonicotinoyl Hydrazone Class Effect on the R2 subunit of Ribonucleotide Reductase," Clinical Cancer Research, vol. 7, pp. 3574-3579, (2001).45, pp. 752-760, (2006). 38

59. Qi G.-F., Yang Z.-Y., and Qin D.-D., Synthesis, characterization and DNA-binding properties of the Cu(II) complex with 7-methoxychromone-3-carbaldehyde-benzoylhydrazone, Chemical and Pharmaceutical Bulletin, vol. 57, pp. 69-73, (2009)